IOP PUBLISHING PHYSICS IN MEDICINE AND BIOLOGY

Phys. Med. Biol. **53** (2008) 5061–5076 doi:10.1088/0031-9155/53/18/014

Fisher information and Shannon entropy for on-line detection of transient signal high-values in laser Doppler flowmetry signals of healthy subjects

Anne Humeau[1,2,4], **Wojciech Trzepizur**[3], **David Rousseau**[2], **François Chapeau-Blondeau**[2] **and Pierre Abraham**[3]

[1] Groupe esaip, 18 rue du 8 mai 1945, BP 80022, 49180 Saint Barthélémy d'Anjou cedex, France
[2] Laboratoire d'Ingénierie des Systèmes Automatisés (LISA), Université d'Angers, 62 avenue Notre Dame du Lac, 49000 Angers, France
[3] Laboratoire de Physiologie et d'Explorations Vasculaires, UMR CNRS 6214-INSERM 771, Centre Hospitalier Universitaire d'Angers, 49033 Angers cedex 01, France

E-mail: ahumeau@esaip.org

Received 15 May 2008, in final form 16 July 2008
Published 22 August 2008
Online at stacks.iop.org/PMB/53/5061

Abstract

Laser Doppler flowmetry (LDF) is an easy-to-use method for the assessment of microcirculatory blood flow in tissues. However, LDF recordings very often present TRAnsient Signal High-values (TRASH), generally of a few seconds. These TRASH can come from tissue motions, optical fibre movements, movements of the probe head relative to the tissue, etc. They often lead to difficulties in signal global interpretations. In order to test the possibility of detecting automatically these TRASH for their removal, we process noisy and noiseless LDF signals with two indices from information theory, namely Fisher information and Shannon entropy. For this purpose, LDF signals from 13 healthy subjects are recorded at rest, during vascular occlusion of 3 min, and during post-occlusive hyperaemia. Computation of Fisher information and Shannon entropy values shows that, when calibrated, these two indices can be complementary to detect TRASH and be insensitive to the rapid increases of blood flow induced by post-occlusive hyperaemia. Moreover, the real-time algorithm has the advantage of being easy to implement and does not require any frequency analysis. This study opens new fields of application for Fisher information and Shannon entropy: LDF 'denoising'.

1. Introduction

Laser Doppler flowmetry (LDF) is a noninvasive method for the assessment of microcirculatory blood flow in tissues. It was first introduced in the 1970's (Riva *et al* 1972, Stern 1975) and has since undergone a continuous development in the theoretical, instrumental and

[4] Author to whom any correspondence should be addressed.

signal processing fields (see for example Binzoni *et al* 2004, 2006, Chao *et al* 2006, Gush *et al* 1984, Humeau *et al* 2004a, 2004b, 2004c, Kvandal *et al* 2006, Li *et al* 2006, Liebert *et al* 2006, Stefanovska *et al* 1999). During LDF measurements, a coherent light is directed, within an optical fibre, towards the tissue under study. Photons that penetrate into the tissue are scattered by moving objects and by static structures. The encounter of moving particles (mainly red blood cells) generates the Doppler effect, modifying the photon frequency. The reemitted light is led, via another optical fibre, towards a photodetector. Optical mixing of light frequency shifted and non-frequency shifted gives rise to a stochastic photocurrent. The tissue blood perfusion signal is extracted from the first moment of the photocurrent fluctuation power spectrum (see for example Humeau *et al* 2007). Yet the LDF technique cannot measure absolute perfusion but has good temporal resolution. Therefore, in clinical research, the technique is best employed to investigate physiological responses to stimuli, such as vascular occlusion followed by reactive hyperaemia (Assous *et al* 2006, Humeau *et al* 2002, Medow *et al* 2007, Rossi *et al* 2007).

Although LDF has led to a growing number of applications for diagnosis purposes, the technique still has some drawbacks. A major problem commonly depicted by clinicians and very often cited in the literature is the presence of TRAnsient Signal High-values (TRASH) that generally have a duration of a few seconds and that can come at any moment during the recordings (Berardesca *et al* 2002, Gush and King 1987, Leahy *et al* 1999, Rajan *et al* 2008, Vongsavan and Matthews 1993). These TRASH generate modifications in the LDF signal values and can lead to difficulties in the signal global interpretation. This is why an accurate detection, and then removal, of TRASH is of great interest for clinicians. However, this detection and removal should be able to differentiate between TRASH and blood flow increases due to post-occlusive hyperaemia, the latter phenomenon containing important physiological information. The TRASH detection is particularly important for poorly compliant subjects or during long-term observations: for these situations, immobility (necessary to avoid TRASH) can be difficult to obtain (Berardesca *et al* 2002, Newson *et al* 1987).

Two indices from information theory, Fisher information and Shannon entropy, have already been useful in the analysis of nonstationary and fluctuating signals in several fields of interest (see for example Jeong *et al* 2006, Martin *et al* 1999). The goal of the present paper is therefore to study the behaviour of these two indices when applied on LDF signals. Can Fisher information and Shannon entropy detect TRASH? Are these two indices from information theory able to discriminate between TRASH and rapidly varying blood flow signals that have their origin in a removal of vascular occlusion (post-occlusive hyperaemia)? Herein, our aim is to analyse the potentialities of Fisher information and Shannon entropy to detect TRASH for their removal. Up to now, some solutions have already been tentatively proposed for TRASH suppression. However, these solutions can be costly and difficult to implement. Fisher information and Shannon entropy are two easy-to-code indices. Therefore, if our results are efficient, the use of the two indices could be an interesting alternative for the TRASH detection in LDF signals.

2. TRASH in LDF measurements

In the LDF technique, TRASH can come from tissue motions, optical fibre movements, movements of the probe head relative to the tissue, etc. No correlation exists *a priori* between the frequency of TRASH and age of the subjects in LDF signals. TRASH generate intensity fluctuations, at the photodetector, similar to the laser Doppler beat frequency. Newson *et al* (1987) demonstrated that the range of frequencies produced in the beat frequency spectrum is 0–3.5 kHz and the magnitude can be much larger than the perfusion related

signal. Moreover, Öberg (1999) analysed the contribution of tissue motion generated by respiratory and circulatory systems of the human body on the LDF signal. His results showed that a flow signal increases linearly with the increase of vibration movements with a constant flow velocity. Furthermore, tissue motion and physical movements of the subjects generate more TRASH in a non-contact measurement technique such as LDF imaging (Karlsson *et al* 2002).

To decrease the presence of TRASH, some authors suggested a modification of the fibre-optic probes (Gush and King 1987), or the conception of integrated probes (de Mul *et al* 1984, Higurashi *et al* 2003, Serov *et al* 2006). Others proposed the use of linearly polarized laser light in combination with a polarization filter for LDF imaging (Karlsson and Wardell 2005). All these techniques can be costly and difficult to implement. An accurate real-time processing of LDF signals from fibre-optic instruments, to detect and then remove TRASH, would be easier, cheaper and of great interest for clinicians.

3. Measurement procedure and signal analysis

3.1. Measurement procedure

In our work, the measurement procedure for LDF signals was the following: thirteen healthy adult men of different ages (43.5 ± 11.3 years old) were studied. The exclusion criteria were: subjects with respiratory or cardiac failure, psychological disorder, hypertension, diabetes, dyslipidemy (treated or untreated), subjects treated with anti-platelet drugs or with non-steroid anti-inflammatory drugs, subjects with chronic inflammatory states (treated or untreated), subjects with a body mass index higher than 35 kg m^{-2}. Moreover, all subjects gave their written informed consent to participate in the study. Furthermore, the institutionally approved study (approval from the local ethical committee) was conducted in accordance with the Declaration of Helsinki. For the signal acquisition, a laser Doppler optical fibre probe (PF408, Perimed, Stockholm, Sweden) connected to a laser Doppler flowmeter (Periflux PF5000, Perimed, Stockholm, Sweden) was positioned on the forearm (ventral face) of the subjects. The probe chosen has a fibre separation of 0.25 mm. Moreover, as our signal processing algorithm is aimed to be used by both clinicians and engineers who would like to analyse and process LDF signals (and thus for whom the human heart synchronous pulsations are of interest), we set the time constant of the laser Doppler flowmeter to 0.2 s. Skin blood flow revealed by LDF signals was assessed in arbitrary units (a.u.) and recorded on a computer via an analogue-to-digital converter (Biopac System) with a sampling frequency of 20 Hz. Recordings were performed with the subjects placed supine in a quiet room with the ambient temperature set at 24 ± 1 °C. After at least 10 min of acclimatization skin blood flow was recorded for several minutes. Then, vascular occlusion was performed by inflating a pressure cuff placed around the upper arm. The cuff was inflated to 200 mmHg for 2.9 min (± 7 s). Then it was released to obtain post-occlusive hyperaemia (see figure 1(a)). During vascular occlusion, a residual signal, called biological zero, exists (see figure 1(a)). It is suggested to originate from Brownian motion and movement of red blood cells (Caspary *et al* 1988, Kernick *et al* 1999, Tenland *et al* 1983). Post-occlusive hyperaemia corresponds to a rapid increase of blood flow occurring after the release of vascular occlusion (see figure 1(a)). Post-occlusive hyperaemia has been the subject of many works for clinical applications and for a better understanding of the blood flow microcirculation (see for example Caspary *et al* 1997, Cracowski *et al* 2006, Wilkin 1987, Yvonne-Tee *et al* 2005, 2006, 2008).

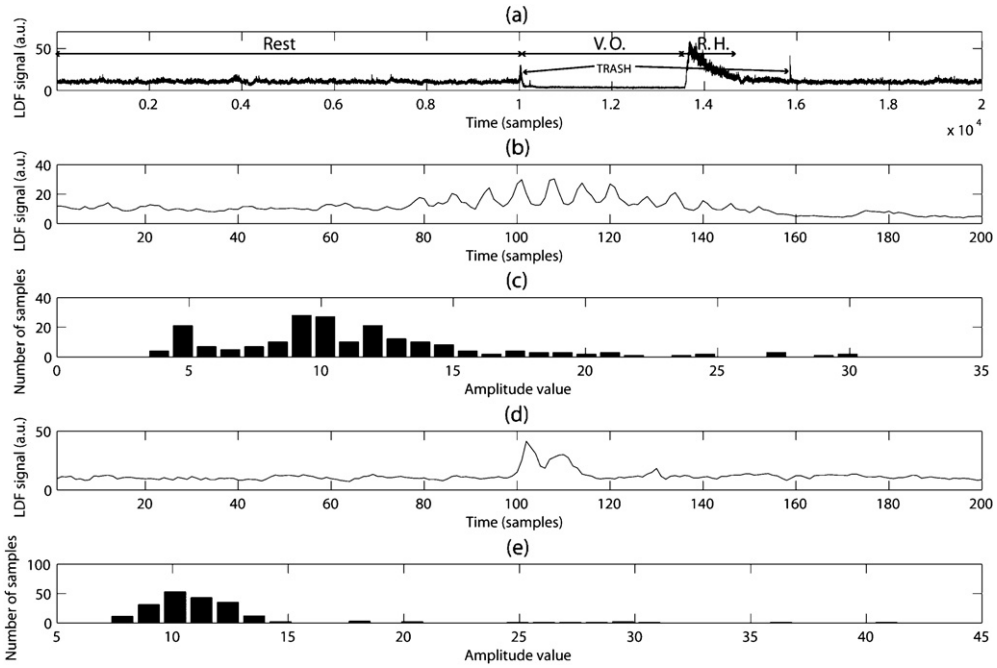

Figure 1. (a) The skin LDF signal recorded on a healthy subject, during rest, vascular occlusion and reactive hyperaemia. V.O. stands for Vascular Occlusion. R.H. stands for Reactive Hyperaemia. (b) First TRASH presented in figure 1(a). (c) Histogram for figure 1(b). The histogram has been computed with $w = 200$ and $N = 30$. (d) Second TRASH presented in figure 1(a). (e) Histogram for figure 1(d). The histogram has been computed with $w = 200$ and $N = 30$.

3.2. Signal analysis

TRASH can occur at any moment during LDF measurements. However, during vascular occlusion, we can note that TRASH very often occur at the beginning of the biological zero. Moreover, TRASH can also occur when no stimulus is used. Therefore, we herein analyse the temporal signature of two kinds of TRASH: the first one corresponds to a TRASH occurring when vascular occlusion starts (at the beginning of the biological zero; see figure 1(b)); the second kind corresponds to a TRASH occurring when recordings are performed at rest (see figure 1(d)). For the temporal signature analysis, we compute the amplitude histogram of LDF signals around the TRASH.

Moreover, herein the 13 LDF signals, that do or do not contain TRASH, are analysed with two indices from information theory. The first index is the Fisher information. The Fisher information $I(t)$ is computed from the probability density function (pdf) of a signal. Thus, let $p(x, t)$ be the pdf of a signal that ranges over $x \in [x_1, x_2]$ at time t, where x_1 and x_2 represent respectively the lower and upper limits of physically meaningful values in the time series. For a signal, at time t, the Fisher information continuous version is defined as (Fisher 1922, Frieden 1998)

$$I(t) = \int_{x_1}^{x_2} \frac{1}{p(x,t)} \left(\frac{\mathrm{d}p(x,t)}{\mathrm{d}x} \right)^2 \mathrm{d}x. \tag{1}$$

$I(t)$ is sensitive to the shape of the pdf (Frieden 2004, Frieden and Soffer 1995). However, due to the derivative term in the integrand of equation (1), the Fisher information is influenced by changes in the local smoothness of $p(x, t)$. Moreover, due to the presence of $1/p(x, t)$ in

the integrand of equation (1), Fisher information is particularly sensitive to the local variations in the low values of the pdf.

In order to compare the results given by the Fisher information with a more commonly used measure, the second index proposed herein to analyse LDF signals is the Shannon entropy. The Shannon entropy is also computed from the pdf of a signal. The continuous version of Shannon entropy $H(t)$ of a signal, at time t, is defined as (Shannon and Weaver 1949)

$$H(t) = -\int_{x_1}^{x_2} p(x,t) \ln p(x,t)\, \mathrm{d}x. \tag{2}$$

$H(t)$ is a measure of randomness. The more random the values of x, the wider the pdf, the larger the value of the Shannon entropy.

We thus computed both Fisher information and Shannon entropy on each part (rest, vascular occlusion and post-occlusive hyperaemia) of LDF signals. For this purpose, the following approach was adopted. First, each LDF signal was binned into sequences of windows, where each window contains w sequential measurements. Then, histograms were generated from the w measurements in each window. Finally, a series of Fisher information and Shannon entropy values were computed from the sequences of histograms.

More precisely, for the first step mentioned above (bins), each LDF signal s was processed in order to obtain a sequence of windows, each one defined as

$$W(m; w; \Delta) = \{s(k), k = 1 + (m-1)\Delta, \ldots, w + (m-1)\Delta\}, \tag{3}$$

where $s(k)$ corresponds to a sample in the signal, m identifies a particular window, w is the number of samples included in each window and Δ determines the degree of overlap between adjacent windows. For the second step (histograms), histograms $p(x_n, m)$ were computed from the samples in the mth window such that the histogram divisions $x_n (n = 1, \ldots, N)$ are spread between the minimum and maximum values of the samples included in the window. For the last step, and from the resulting histograms, Fisher information and Shannon entropy were respectively determined as

$$I(m) = \sum_{n=1}^{N} \frac{[p(x_{n+1}, m) - p(x_n, m)]^2}{p(x_n, m)}, \tag{4}$$

$$H(m) = -\sum_{n=1}^{N} p(x_n, m) \ln p(x_n, m). \tag{5}$$

4. Results and discussion

In our work, we first analysed the temporal signature of two TRASH. As shown in the figures presented thereafter, TRASH can lead to signal increases that are lower, higher or in the same amplitude range as those generated by post-occlusive hyperaemia. That is why the development of an automatic and inline algorithm able to differentiate TRASH from post-occlusive hyperaemia is not an easy task. Two histograms corresponding to the two kinds of TRASH presented above (a TRASH occurring at the beginning of a biological zero and a TRASH occurring at rest) are shown in figures 1(c) and (e). From these histograms, we observe that, for the first kind of TRASH (see figures 1(b) and (c)), most LDF samples have an amplitude around 10, and few of them have amplitudes higher than 10. The results are the same for the second kind of TRASH (see figures 1(c) and (e)), except that for the latter case the histogram has a width narrower than the previous one. Furthermore, the temporal duration of

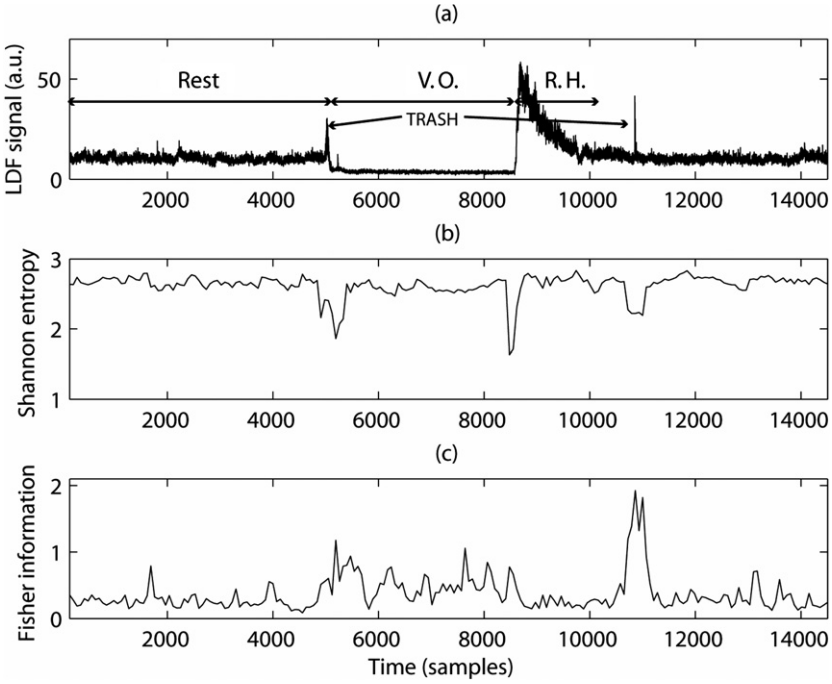

Figure 2. (a) The skin LDF signal recorded on a healthy subject, during rest, vascular occlusion and reactive hyperaemia. V.O. stands for Vascular Occlusion. R.H. stands for Reactive Hyperaemia. (b) Corresponding Shannon entropy computed with $w = 300$, $\Delta = 70$ and $N = 20$. (c): Corresponding Fisher information computed with $w = 300$, $\Delta = 70$ and $N = 20$.

the second kind of TRASH is shorter than that of the first kind. However, in both cases, TRASH last only a few seconds. Some authors suggested that the TRASH occurring at the beginning of a biological zero come from the displacement of arterial blood by cuff compression (Kernick *et al* 1999).

We then investigated the behaviour of Fisher information and Shannon entropy on LDF signals with and without TRASH. For this purpose, we first studied the influence of the window size w, the overlap Δ, and the histogram resolution N on Fisher information and Shannon entropy values. Through this analysis, we wanted to answer the question: does it exist sets of parameters that allow the detection of TRASH and, at the same time, that lead to indices insensitive to blood flow increases induced by post-occlusive hyperaemia?

From our computations, we observe that Shannon entropy computed with the set of values $w = 300$, $\Delta = 70$ and $N = 20$, is able to detect TRASH but can also be sensitive to post-occlusive hyperaemia (see figures 2(a) and (b), figures 3(a) and (b) and figures 4(a) and (b)). In this case, a differentiation between a physiological blood flow increase due to the removal of vascular occlusion and TRASH is not an easy task. However, the Fisher information computed with the same parameters is able to detect some TRASH and can be insensitive to post-occlusive hyperaemia (see figures 2(a) and (c), figures 3(a) and (c) and figures 4(a) and (c)).

In order to analyse these results we show, in figures 5(a) and (b), a window containing the last TRASH presented in figure 2(a) and the corresponding histogram. Moreover, figures 5(c) and (d) show, respectively, a window containing the beginning of post-occlusive hyperaemia presented in figure 2(a), and the corresponding histogram. The beginning of

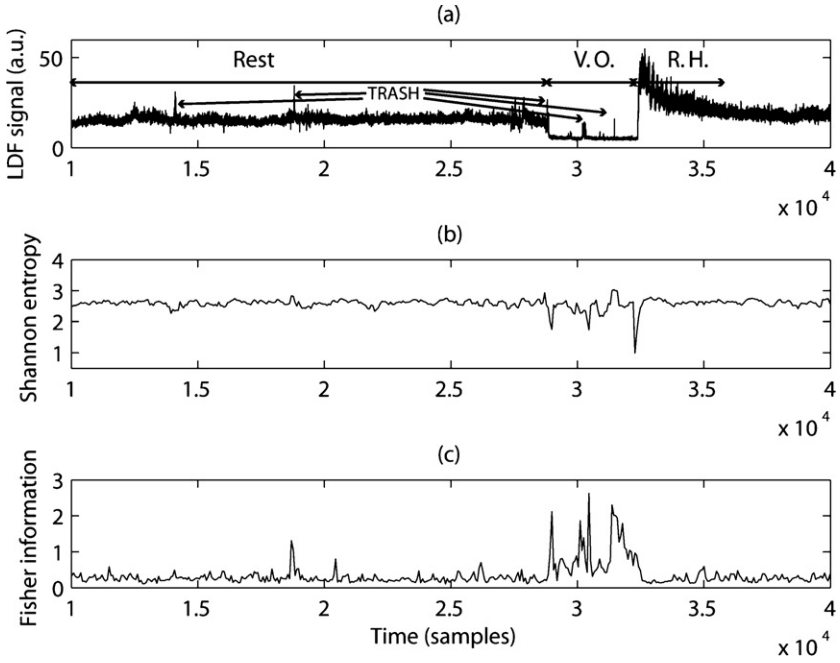

Figure 3. Same as figure 2 for another LDF signal.

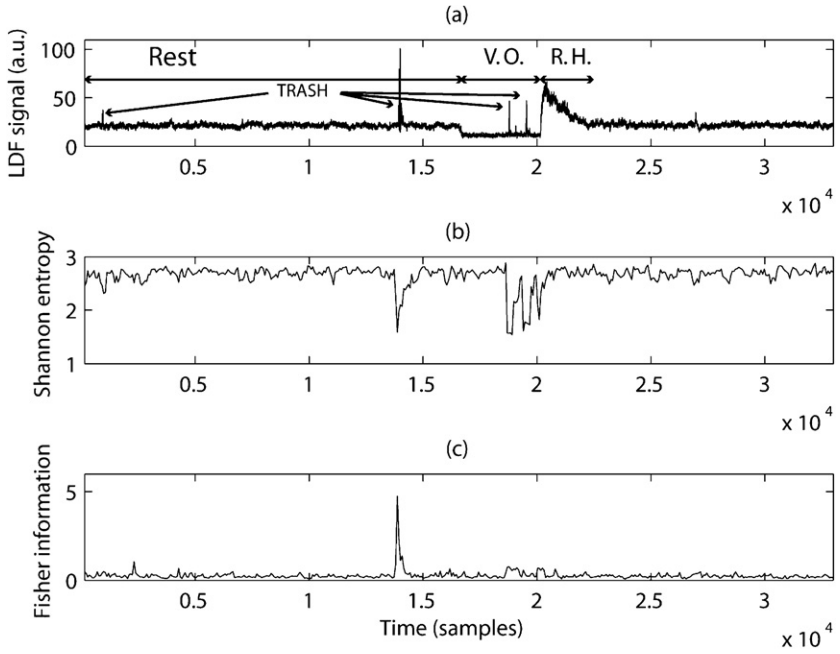

Figure 4. Same as figure 2 for another LDF signal.

reactive hyperaemia is of interest here as it corresponds to a very rapid increase of the LDF signal as that observed during TRASH. From figure 5(d), we note that the histogram of the beginning of reactive hyperaemia, after a symmetry, has a shape quite similar to that of the

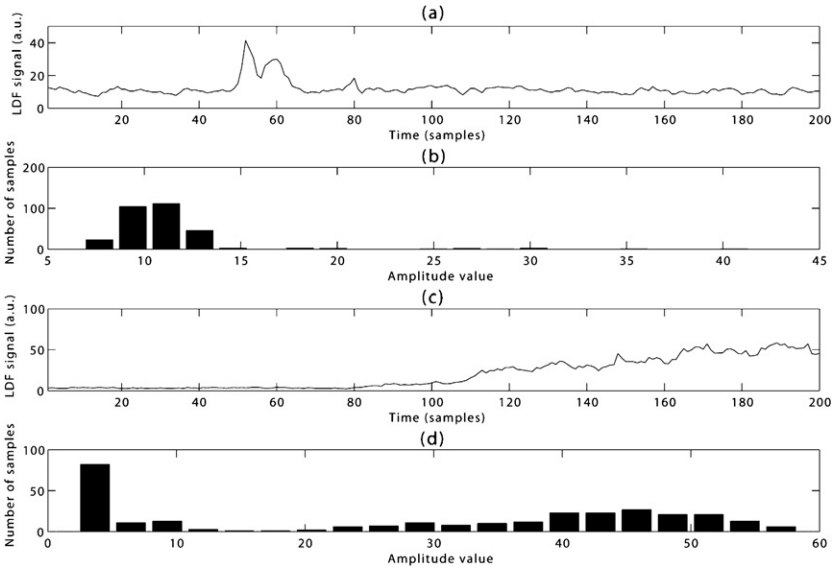

Figure 5. (a) A window containing the last movement artefact presented in figure 2(a). (b) Histogram for figure 5(a). The histogram has been computed with $w = 300$ and $N = 20$. (c) A window containing the beginning of the reactive hyperaemia presented in figure 2(a). (d) Histogram for figure 5(c). The histogram has been computed with $w = 300$ and $N = 20$.

TRASH presented in figure 5(b). That is why Shannon entropy reacts in nearly the same way for reactive hyperaemia and for TRASH (see figure 2(b)). However, the Fisher information definition containing a derivative term and a term $1/p(x, t)$ (see equation (1)) is influenced by changes in the local smoothness of the pdf and by the local variations in the low values of the pdf. That is why, for the parameters mentioned above, it is able to differentiate TRASH from post-occlusive hyperaemia.

In order to obtain Shannon entropy values which are able to behave differently for TRASH and for reactive hyperaemia, we have to obtain histograms with different shapes for the two signals increases. For this purpose, we suggest to shorten the width of the window w. Thus, for a window width shorter than the full LDF amplitude variation observed at the beginning of reactive hyperaemia, the histograms obtained for TRASH and for post-occlusive hyperaemia will be different.

Following this methodological approach, we computed the Shannon entropy with $w = 50$, and proposed to maintain the ratio w/Δ and w/N as above: w/Δ around 4, and w/N near 15. This led us to choose $\Delta = 12$ and $N = 3$. From these choices, the results show that Shannon entropy allows the detection of TRASH and is nearly insensitive to post-occlusive hyperaemia (see figures 6(a) and (b), 7(a) and (b) and 8(a) and (b)). For these parameter values, the histograms obtained for TRASH and for a beginning of post-occlusive hyperaemia are shown in figure 9. The shape of the two histograms are, this time, different. That is why, for the new set of parameters, Shannon entropy shows a different behaviour for TRASH and for a post-occlusive hyperaemia.

We then analysed the influence of Δ and N values on the results. For Δ analysis, we computed Shannon entropy with the following parameter values: $w = 50$, $\Delta = 5$, $N = 3$, and then $w = 50$, $\Delta = 40$, and $N = 3$. We also computed Fisher information with the following parameters: $w = 300$, $\Delta = 10$, $N = 20$, and then $w = 300$, $\Delta = 130$, $N = 20$. The results

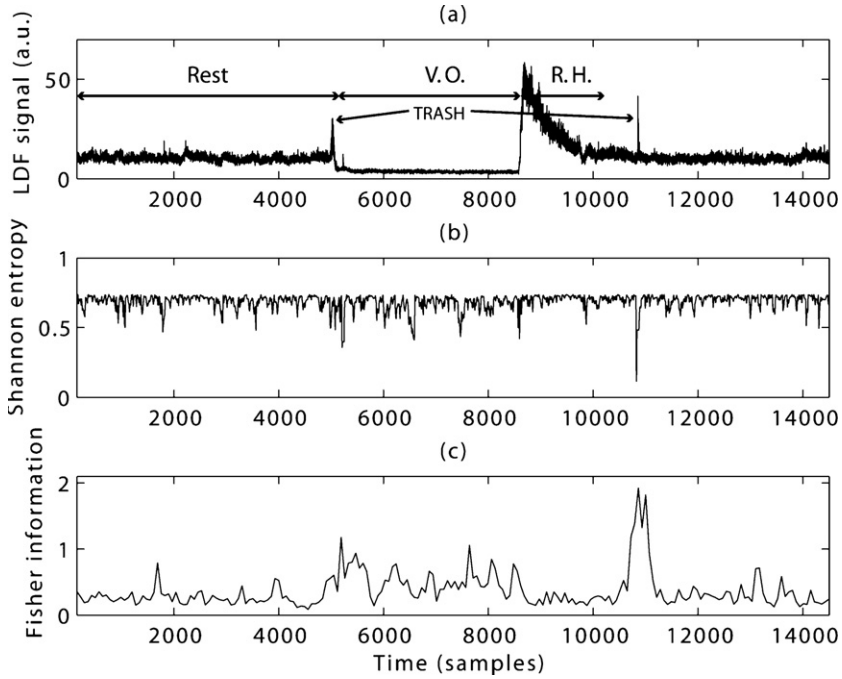

Figure 6. (a) and (c) Same as figure 2(a) and (c), respectively. (b) Same as figure 2(b) except that $w = 50$, $\Delta = 12$ and $N = 3$ are chosen for the computation of Shannon entropy.

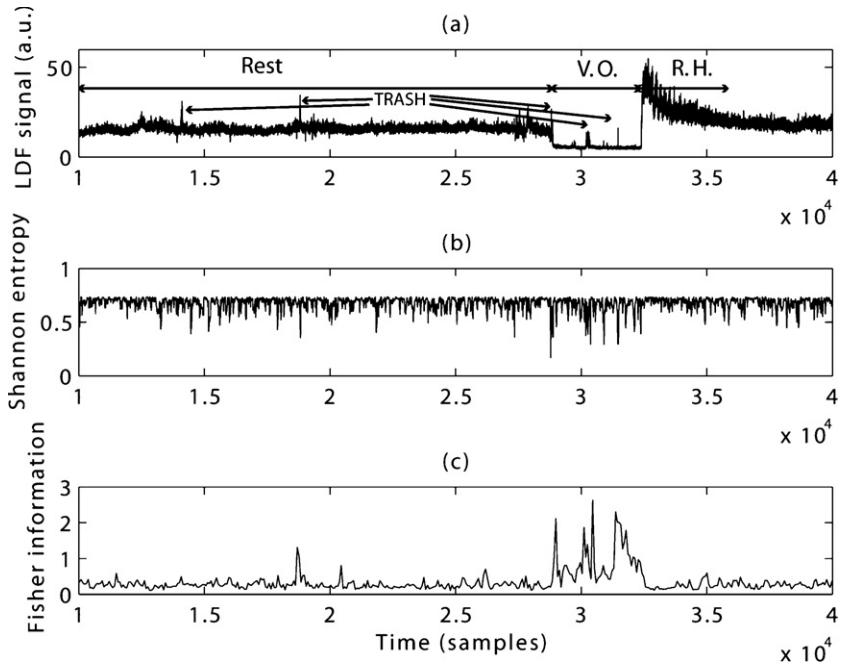

Figure 7. (a) and (c) Same as figure 3(a) and (c), respectively. (b) Same as figure 3(b) except that $w = 50$, $\Delta = 12$ and $N = 3$ are chosen for the computation of Shannon entropy.

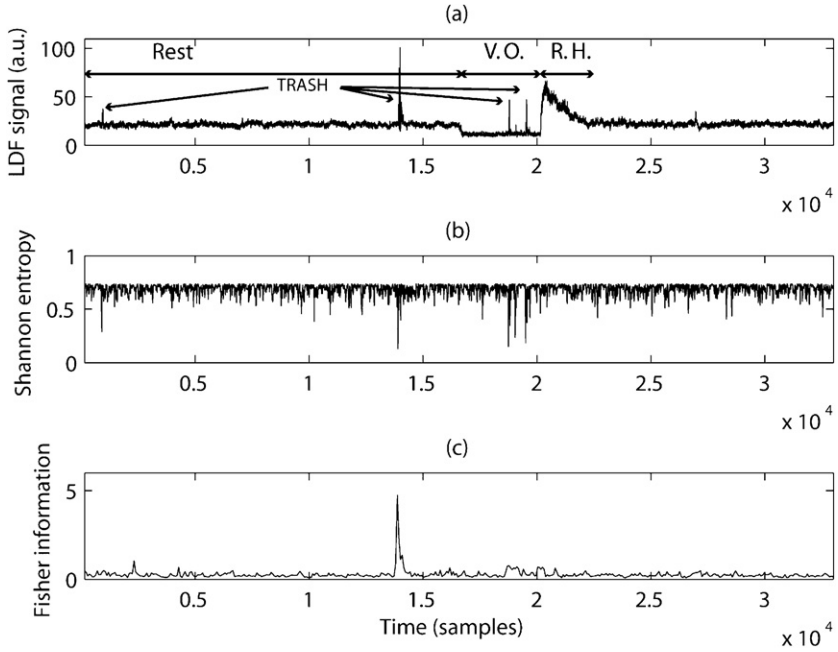

Figure 8. (a) and (c) Same as figure 4(a) and (c), respectively. (b) Same as figure 4(b) except that $w = 50$, $\Delta = 12$ and $N = 3$ are chosen for the computation of Shannon entropy.

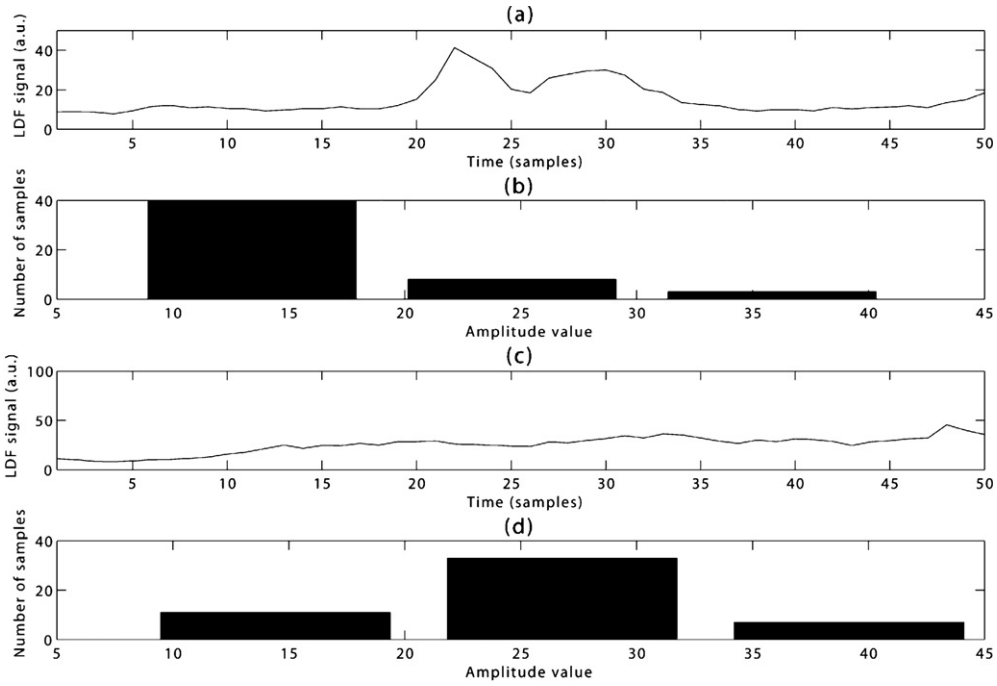

Figure 9. (a) A window containing the last movement artefact presented in figure 2(a). (b) Histogram for figure 9(a). The histogram has been computed with $w = 50$ and $N = 3$. (c) A window containing the beginning of the reactive hyperaemia presented in figure 2(a). (d) Histogram for figure 9(c). The histogram has been computed with $w = 50$ and $N = 3$.

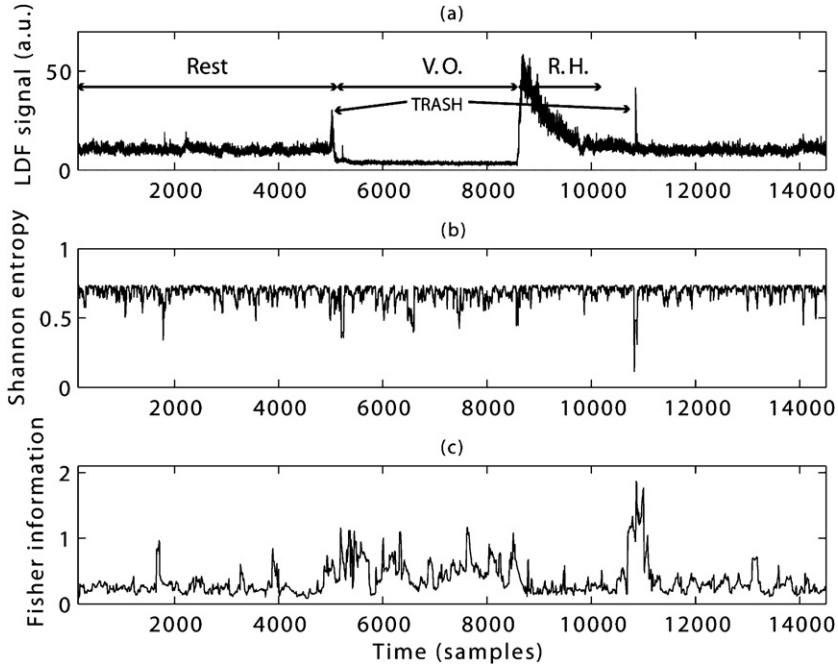

Figure 10. (a) Same as figure 2(a). (b) Corresponding Shannon entropy computed with $w = 50$, $\Delta = 5$, $N = 3$. (c) Corresponding Fisher information computed with $w = 300$, $\Delta = 10$, $N = 20$.

are presented in figures 10 and 11. The latter figures associated with figure 6 show that the wider the value of Δ, the smoother the signals representing the Shannon entropy and Fisher information. When these signals become very smooth, an accurate detection of the TRASH *localization* can become a difficult task. After several tests and in order to accurately localize TRASH, we suggest to use $\Delta = 12$ for the Shannon entropy, and $\Delta = 70$ for the Fisher information. For the analysis of N influence, we computed the Shannon entropy with the following parameter values: $w = 50$, $\Delta = 12$, $N = 2$, and then $w = 50$, $\Delta = 12$, and $N = 10$. We also computed the Fisher information with the following parameters: $w = 300$, $\Delta = 70$, $N = 5$, and then $w = 300$, $\Delta = 70$, $N = 100$. The results are presented in figures 12 and 13. The latter figures associated with figure 6 show that the larger the value of N, the smoother the signals representing Shannon entropy and Fisher information and the wider the peaks due TRASH. We also note that the mean values of the signals vary when N varies. When Shannon entropy and Fisher information signals become very smooth and when their peaks are wide, an accurate detection of the TRASH *localization* can become a difficult task. After several tests and in order to have an accurate localization of the TRASH, we propose to choose $N = 3$ for the Shannon entropy, and $N = 20$ for the Fisher information.

From these results, and as far as the LDF TRASH detection is concerned, we suggest to use $w = 50$, $\Delta = 12$, and $N = 3$, for Shannon entropy computation, and $w = 300$, $\Delta = 70$, and $N = 20$, for the Fisher information index (see figures 6–8; these suggestions take into account a signal sampling frequency of 20 Hz). We then propose to consider an increase in the measured signal as TRASH when one (or both) of the two indices, computed with the above-mentioned sets of values, varies more than a fixed percentage from its basal value: decrease of more than 43% for Shannon entropy and increase of more than 600% for Fisher information, for example. This could lead to the discrimination of TRASH from post-occlusive hyperaemia in

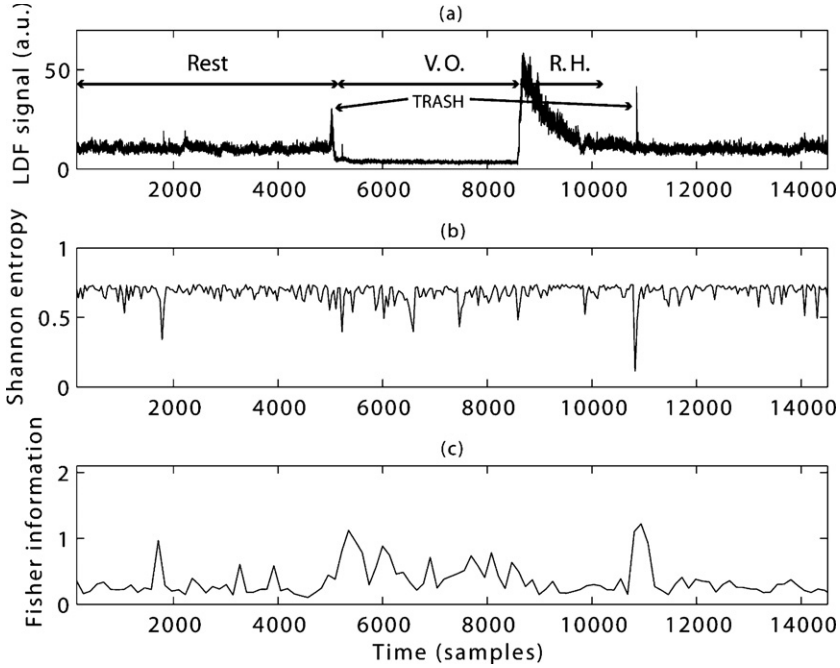

Figure 11. (a) Same as figure 2(a). (b) Corresponding Shannon entropy computed with $w = 50$, $\Delta = 40$, $N = 3$. (c) Corresponding Fisher information computed with $w = 300$, $\Delta = 130$, $N = 20$.

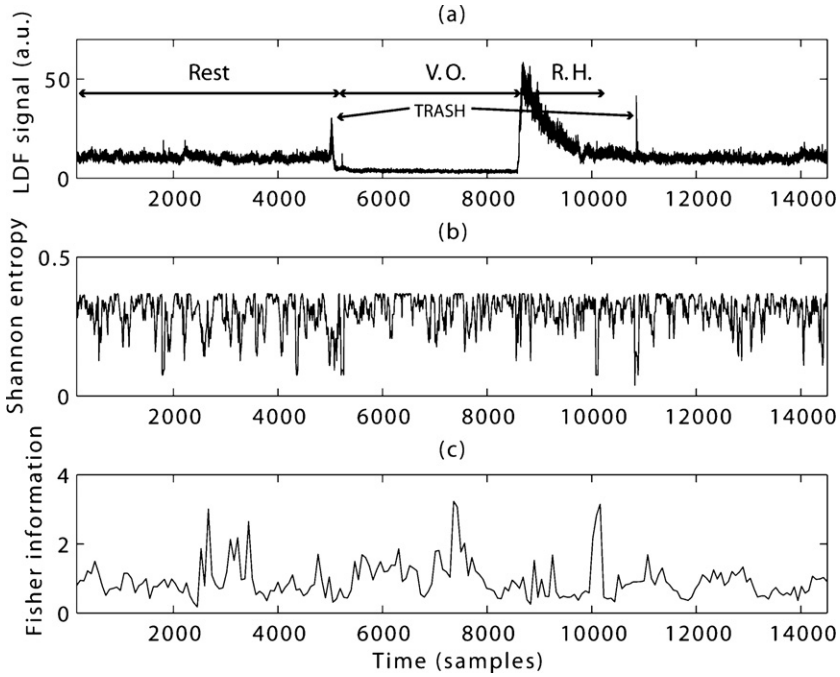

Figure 12. (a) Same as figure 2(a). (b) Corresponding Shannon entropy computed with $w = 50$, $\Delta = 12$, $N = 2$. (c) Corresponding Fisher information computed with $w = 300$, $\Delta = 70$, $N = 5$.

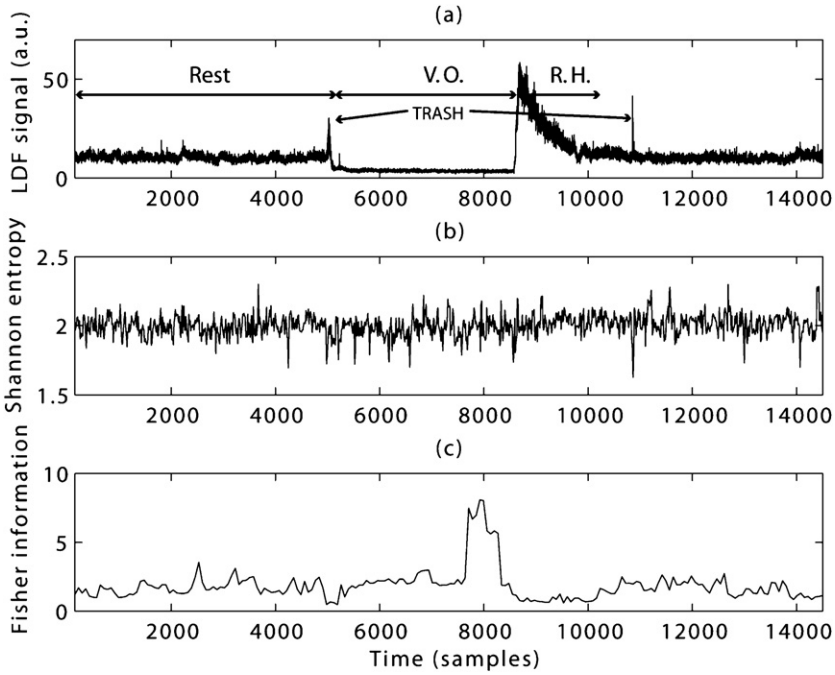

Figure 13. (a) Same as figure 2(a). (b) Corresponding Shannon entropy computed with $w = 50$, $\Delta = 12$, $N = 10$. (c) Corresponding Fisher information computed with $w = 300$, $\Delta = 70$, $N = 100$.

healthy subjects. Moreover, in order to increase the accuracy of the differentiation between TRASH and post-occlusive hyperaemia, a comparison of the LDF signal mean value between the current window with the previous window could be added (reactive hyperaemia would lead to an increase of the mean value in the current window compared to the previous window, whereas TRASH would probably have a very limited impact over the mean value). From figures 6–8, we observe that Shannon entropy and Fisher information can be complementary to distinguish TRASH from very rapid increases in blood flow induced by the release of vascular occlusion. Moreover, after TRASH are detected, a short period (for example a few seconds) 'eye close' scheme could be introduced (replacement by the previous seconds of signal) to remove the erroneous signal samples. The latter proposal is based on the fact that TRASH normally die out after a period of a few seconds (TRASH duration may vary; the TRASH presented in figures 6–8 have a duration between 0.35 and 8 s). Otherwise, after TRASH are detected, an indication mentioning that this part of signal has a high probability of being noisy could also be chosen.

For a given length of vascular occlusion, post-occlusive hyperaemia of healthy subjects have a shape that is different from those observed for peripheral arterial obliterative disease (PAOD) patients (Humeau *et al* 2000, 2002). Thus, Östergren *et al* (1988) found a biphasic response in PAOD patients, whereas Ray *et al* (1999) noted that three patterns can be observed (immediate large amplitude peak following reperfusion; multiple large amplitude peaks with delay in the highest peak; and gradual increase of the signal but no large amplitude peaks). Moreover, PAOD subjects present a time to highest peak abnormally prolonged after the release of the occlusion (Kvernebo *et al* 1989, del Guercio *et al* 1986, Östergren *et al* 1988). Therefore, in the case of PAOD patients, our algorithm for Shannon entropy would give even more accurate results for this pathologic population: the reactive hyperaemia increase in a

window of 50 samples width would be much lower than for healthy subjects. In this case, the differentiation between TRASH and a blood flow increase due to post-occlusive hyperaemia is expected to be more efficient.

Moreover, studying post-occlusive hyperaemia, Wilkin (1987) has shown that the longer the vascular occlusion, the lower the rate of rise to peak flow and the higher the maximum value of the flow. This means that for lengths of occlusion shorter than that used in our work, our algorithm could give less accurate results. However, a work has recommended that studies using post-occlusive forearm skin hyperaemia should occlude the forearm for at least 3 min (Yvonne-Tee *et al* 2004). As a consequence, our work could be efficient for clinical applications following the latter recommendation.

5. Conclusion

The LDF technique relies on the measurement of the Doppler shifts induced by the interactions between photons of a laser light and moving blood cells of the microcirculation. However, LDF data very often contain TRASH that can lead to difficulties in signal global interpretations. Our work analysed the temporal signature of two kinds of TRASH. Moreover, we have demonstrated that two information theory indices, Fisher information and Shannon entropy, could discriminate TRASH from a measurement protocol where a very rapid increase in blood flow is expected (release of a pressure cuff occluding blood flow). In opposition to other TRASH algorithms that have been proposed in some patents, the two indices proposed herein have the advantage of being simple as they do not require any frequency analysis of the photocurrent for their implementation. Moreover, their use can lead to a real-time process of LDF signals. Information theory can thus be of interest to improve the processing and understanding of complex biomedical signals. Other information indices could also be analysed for the TRASH detection and for their characterization. A Bayesian technique or receiver operating characteristic curves could then be proposed as a validation approach.

References

Assous S, Humeau A, Tartas M, Abraham P and L'Huillier J P 2006 S-transform applied to laser Doppler flowmetry reactive hyperemia signals *IEEE Trans. Biomed. Eng.* **53** 1032–37

Berardesca E, Lévêque J L, Masson P and EEMCO Group 2002 EEMCO guidance for the measurement of skin microcirculation *Skin Pharmacol. Appl. Skin Physiol.* **15** 442–56

Binzoni T, Leung T S, Seghier M L and Delpy D T 2004 Translational and Brownian motion in laser-Doppler flowmetry of large tissue volumes *Phys. Med. Biol.* **49** 5445–58

Binzoni T, Leung T S, Rüfenacht D and Delpy D T 2006 Absorption and scattering coefficient dependence of laser-Doppler flowmetry models for large tissue volumes *Phys. Med. Biol.* **51** 311–33

Caspary L, Creutzig A and Alexander K 1988 Biological zero in laser Doppler fluximetry *Int. J. Microcirc. Clin. Exp.* **7** 367–71

Caspary L, Nordbruch S, Lange R and Creutzig A 1997 Circadian variation of skin perfusion in arterial occlusive disease *VASA* **26** 194–8

Chao P T, Jan M Y, Hsiu H, Hsu T L, Wang W K and Lin Wang Y Y 2006 Evaluating microcirculation by pulsatile laser Doppler signal *Phys. Med. Biol.* **51** 845–54

Cracowski J L, Kom G D, Salvat-Melis M, Renversez J C, McCord G, Boignard A, Carpentier P H and Schwedhelm E 2006 Postocclusive reactive hyperemia inversely correlates with urinary 15-F2t-isoprostane levels in systemic sclerosis *Free Radic. Biol. Med.* **40** 1732–7

de Mul F F M, van Spijker J, van der Plas D, Greve J, Aarnoudse J G and Smits T M 1984 Mini laser-Doppler (blood) flow monitor with diode laser source and detection integrated in the probe *Appl. Opt.* **23** 2970–73

del Guercio R F, Leonardo G and Arpaia M R 1986 Evaluation of postischemic hyperemia on the skin using laser Doppler velocimetry: study on patients with claudicatio intermittens *Microvasc. Res.* **32** 289–99

Fisher R A 1922 On the mathematical foundations of theoretical statistics *Phil. Trans. R. Soc. Lond.* A **222** 309–68

Frieden B R 1998 *Physics from Fisher Information: A Unification* (UK: Cambridge University Press)
Frieden B R and Soffer B H 1995 Lagrangians of physics and the game of Fisher-information transfer *Phys. Rev.* E **52** 2274–86
Frieden B R 2004 *Science from Fisher Information: A Unification* (UK: Cambridge University Press)
Gush R J and King T A 1987 Investigation and improved performance of optical fiber probes in laser Doppler blood flow measurement *Med. Biol. Eng. Comput.* **25** 391–6
Gush R J, King T A and Jayson M I 1984 Aspects of laser light scattering from skin tissue with application to laser Doppler blood flow measurement *Phys. Med. Biol.* **29** 1463–76
Higurashi E, Sawada R and Ito T 2003 An integrated laser blood flowmeter *J. Lightwave Technol.* **21** 591–5
Humeau A, Fizanne L, Garry A, Saumet J L and L'Huillier J P 2004a Signal processing methodology to study the cutaneous vasodilator response to a local external pressure application detected by laser Doppler flowmetry *IEEE Trans. Biomed. Eng.* **51** 190–2
Humeau A, Koïtka A, Abraham P, Saumet J L and L'Huillier J P 2004b Time-frequency analysis of laser Doppler flowmetry signals recorded in response to a progressive pressure applied locally on anaesthetised healthy rats *Phys. Med. Biol.* **49** 843–57
Humeau A, Koïtka A, Abraham P, Saumet J L and L'Huillier J P 2004c Spectral components of laser Doppler flowmetry signals recorded in healthy and type 1 diabetic subjects at rest and during a local and progressive cutaneous pressure application: scalogram analyses *Phys. Med. Biol.* **49** 3957–70
Humeau A, Koïtka A, Saumet J L and L'Huillier J P 2002 Wavelet de-noising of laser Doppler reactive hyperemia signals to diagnose peripheral arterial occlusive diseases *IEEE Trans. Biomed. Eng.* **49** 1369–71
Humeau A, Saumet J L and L'Huillier J P 2000 Use of wavelets to accurately determine parameters of laser Doppler reactive hyperemia *Microvasc. Res.* **60** 141–8
Humeau A, Steenbergen W, Nilsson H and Strömberg T 2007 Laser Doppler perfusion monitoring and imaging: novel approaches *Med. Biol. Eng. Comput.* **45** 421–35
Jeong Y, Sanders B F and Grant S B 2006 The information content of high-frequency environmental monitoring data signals pollution events in the coastal ocean *Environ. Sci. Technol.* **40** 6215–20
Karlsson M G D, Larsson M, Strömberg T and Wardell K 2002 Influence of tissue movements on laser Doppler perfusion imaging *Proc. SPIE* **4624** 106–14
Karlsson M G D and Wardell K 2005 Polarized laser Doppler perfusion imaging—a reduction of movement-induced artifacts *J. Biomed. Opt.* **10** 064002
Kernick D P, Tooke J E and Shore A C 1999 The biological zero signal in laser Doppler fluximetry—origins and practical implications *Pflugers Arch.* **437** 624–31
Kvandal P, Landsverk S A, Bernjak A, Stefanovska A, Kvernmo H D and Kirkeboen K A 2006 Low-frequency oscillations of the laser Doppler perfusion signal in human skin *Microvasc. Res.* **72** 120–7
Kvernebo K, Slagsvold C E and Stranden E 1989 Laser Doppler flowmetry in evaluation of skin post-ischaemic reactive hyperaemia. A study in healthy volunteers and atherosclerotic patients *J. Cardiovasc. Surg.* **30** 70–5
Leahy M J, de Mul F F M, Nilsson G E and Maniewski R 1999 Principles and practice of the laser-Doppler perfusion technique *Technol. Health Care* **7** 143–62
Li Z, Tam E W, Kwan M P, Mak A F, Lo S C and Leung M C 2006 Effects of prolonged surface pressure on the skin blood flowmotions in anaesthetized rats-an assessment by spectral analysis of laser Doppler flowmetry signals *Phys. Med. Biol.* **51** 2681–94
Liebert A, Zołek N and Maniewski R 2006 Decomposition of a laser-Doppler spectrum for estimation of speed distribution of particles moving in an optically turbid medium: Monte Carlo validation study *Phys. Med. Biol.* **51** 5737–51
Martin M T, Pennini F and Plastino A 1999 Fisher's information and the analysis of complex signals *Phys. Lett.* A **256** 173–80
Medow M S, Taneja I and Stewart J M 2007 Cyclooxygenase and nitric oxide synthase dependence of cutaneous reactive hyperemia in humans *Am. J. Physiol. Heart Circ. Physiol.* **293** H425–32
Newson T P, Obeid A N, Wolton R S, Boggett D and Rolfe P 1987 Laser-Doppler velocimetry: the problem of movement artifact *J. Biomed. Eng.* **9** 169–72
Öberg P A 1999 Tissue motion—a disturbance in the laser-Doppler blood flow signal? *Technol. Health Care* **7** 185–92
Östergren J, Schöps P and Fagrell B 1988 Evaluation of a laser Doppler multiprobe for detecting skin microcirculatory disturbances in patients with obliterative arteriosclerosis *Int. Angiol.* **7** 37–41
Rajan V, Varghese B, van Leeuwen T G and Steenbergen W 2008 Review of methodological developments in laser Doppler flowmetry *Lasers Med. Sci.* doi: 10.1007 /s10103–007-0524–0
Ray S A, Buckenham T M, Belli A M, Taylor R S and Dormandy J A 1999 The association between laser Doppler reactive hyperaemia curves and the distribution of peripheral arterial disease *Eur. J. Vasc. Endovasc. Surg.* **17** 245–8

Riva C, Ross B and Benedek G B 1972 Laser Doppler measurements of blood flow in capillary tubes and retinal arteries *Invest. Ophthalmol.* **11** 936–44

Rossi M, Carpi A, Di Maria C, Franzoni F, Galetta F and Santoro G 2007 Post-ischaemic peak flow and myogenic flowmotion component are independent variables for skin post-ischaemic reactive hyperaemia in healthy subjects *Microvasc. Res.* **74** 9–14

Serov A N, Nieland J, Oosterbaan S, de Mul F F M, van Kranenburg H, Bekman H H P T and Steenbergen W 2006 Integrated optoelectronic probe including a vertical cavity surface emitting laser for laser Doppler perfusion monitoring *IEEE Trans. Biomed. Eng.* **53** 2067–74

Shannon C and Weaver W 1949 *The Mathematical Theory of Communication* (Urbana, IL: University of Illinois Press)

Stefanovska A, Bracic M and Kvernmo H D 1999 Wavelet analysis of oscillations in the peripheral blood circulation measured by laser Doppler technique *IEEE Trans. Biomed. Eng.* **46** 1230–9

Stern M D 1975 *In vivo* evaluation of microcirculation by coherent light scattering *Nature* **254** 56–8

Tenland T, Salerud E G, Nilsson G E and Oberg P A 1983 Spatial and temporal variations in human skin blood flow *Int. J. Microcirc. Clin. Exp.* **2** 81–90

Vongsavan N and Matthews B 1993 Some aspects of the use of laser Doppler flow meters for recording tissue blood flow *Exp. Physiol.* **78** 1–14

Wilkin J K 1987 Cutaneous reactive hyperemia: viscoelasticity determines response *J. Invest. Dermatol.* **89** 197–200

Yvonne-Tee G B, Rasool A H G, Halim A S and Rahman A R A 2004 Dependence of human forearm skin postocclusive reactive hyperemia on occlusion time *J. Pharmacol. Toxicol. Methods* **50** 73–8

Yvonne-Tee G B, Rasool A H G, Halim A S and Rahman A R A 2005 Reproducibility of different laser Doppler fluximetry parameters of postocclusive reactive hyperemia in human forearm skin *J. Pharmacol. Toxicol. Methods* **52** 286–92

Yvonne-Tee G B, Rasool A H, Halim A S and Rahman A R 2006 Noninvasive assessment of cutaneous vascular function in vivo using capillaroscopy, plethysmography and laser-Doppler instruments: its strengths and weaknesses *Clin. Hemorheol. Microcirc.* **34** 457–73

Yvonne-Tee G B, Rasool A H G, Halim A S, Wong A R and Rahman A R A 2008 Method optimization on the use of postocclusive hyperemia model to assess microvascular function *Clin. Hemorheol. Microcirc.* **38** 119–33